Reliability Engineering and System Safety 232 (2023) 109071

Contents lists available at ScienceDirect

Reliability Engineering and System Safety

journal homepage: www.elsevier.com/locate/ress

Characterizing resilience of flood-disrupted dynamic transportation network through the lens of link reliability and stability

Shangjia Dong [a,*], Xinyu Gao [b], Ali Mostafavi [b], Jianxi Gao [c], Utkarsh Gangwal [a]

[a] Department of Civil and Environmental Engineering, Disaster Research Center, University of Delaware, Newark, DE 19716, United States of America
[b] Zachry Department of Civil and Environmental Engineering, Texas A&M University, College Station, TX, 77843, United States of America
[c] Computer Science Department & Network Science and Technology Center, Rensselaer Polytechnic Institute, Troy, NY, 12180, United States of America

ARTICLE INFO

Keywords:
Urban flooding
Traffic reliability
Link stability
Transportation network resilience

ABSTRACT

Traffic congestion occurs daily but the transportation network still functions to meet people's travel needs. We propose that a road meets operation requirements as long as the quality of its links (i.e., speed or travel time) satisfies an acceptable threshold. This paper incorporates the link reliability concept into the road travel performance using the link quality threshold to offer new perspectives on network resilience measurement. We introduce two aggregated macroscopic metrics: network reliability scale index, and network stability, based on the link reliability to quantify the road travel performance change in facing external disturbance. We use the temporal traffic-embedded Harris County, TX transportation network during the 2017 Hurricane Harvey as a case study. We show that the proposed metrics can well capture the transportation network performance variation during flooding. Also, we develop an integrated resilience metric that encapsulates the network resistance, recoverability, and rapidity in facing flooding. The results move us closer to better understanding transportation network resilience behavior in different link quality conditions (q). The findings of this research also provide important insights for city planners and traffic operators to examine transportation network resilience through a reliability and stability lens.

1. Introduction

Transportation networks are the backbone of human movements and activities in urban systems. Maintaining road network topological integrity in facing disturbances is critical for providing basic transport functionality [1]. Extensive research has already been devoted to road network resilience assessment using topological information of physical roads as it is the most accessible and complete data source. For example, Dong et al. [2] investigated the robustness of co-located road and sewer networks in different earthquake disruption scenarios. Wang et al. [3] examined the road network connectivity in the face of flood-induced large-scale inundation. Topology-based network robustness [4,5] modeling and analysis have revealed different important patterns and governing characteristics of road network structure in various disaster disruption scenarios, which can help inform vulnerability reduction and hazard mitigation strategies [6–8]. However, the topological integrity of the road network does not fully guarantee the desired level of travel performance. Functionality loss such as heavy congestion can also lead to transportation network failure. More importantly, these two types of failures are often compounded during disasters such as flooding and further exacerbate the impact of flooding on transportation resilience. Using the traffic network of Harris County, Texas (USA), in the context of the 2017 Hurricane Harvey as an example, Fig. 1(a) shows the spatial mapping of the proportion of the time that a road is congested from 8 am to 9 am on both August 8th and 28th, 2017. Fig. 1(b) presents the mapping of the congestion time ratio difference between them, which encapsulates the impact of Hurricane Harvey flooding on road congestion.

To reveal the transportation resilience behavior, we use a link quality measure to characterize the travel performance. The proportion of the time that the link quality meets functionality expectations is considered the link reliability. We hypothesize that the link reliability of a network follows a power-law distribution and can help us capture the network resilience behavior during flood disruptions. Moreover, although link reliability varies over time, we expect the link reliability variation to fluctuate within a range to ensure stable travel performance. However, as shown in Fig. 1(b), the increase or decrease in reliability of certain links was extreme. Such abnormal increase and decrease would induce perturbations and result in the shift in the network metastable states [9]. We propose that link reliability variation reflects the network stability behavior and can be used to further

* Corresponding author.
E-mail address: sjdong@udel.edu (S. Dong).

https://doi.org/10.1016/j.ress.2022.109071
Received 6 March 2022; Received in revised form 20 September 2022; Accepted 26 December 2022
Available online 29 December 2022
0951-8320/

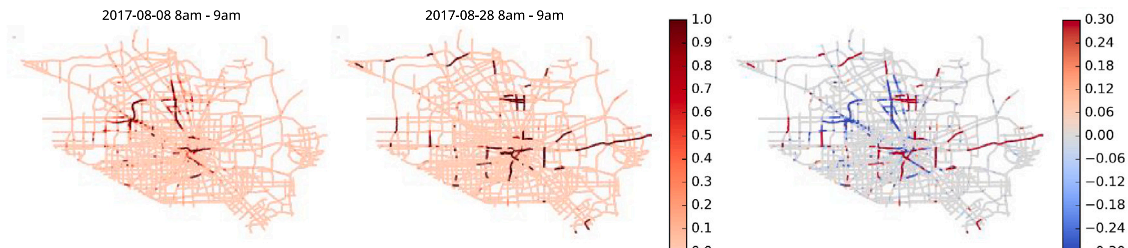

(a) Congestion time ratio　　(b) Congestion time ratio difference

Fig. 1. Dynamic link reliability of Harris County, TX transportation network.

characterize the network resilience performance beyond topological characteristics.

It is often anticipated that network performance will experience degradation during flooding, but exactly how long it takes to recover and the extent to which the network performance will be disrupted remains unknown. The hypothesis and research questions presented above motivate us to understand the network resilience behavior through the lens of link reliability and stability in the face of disaster disruptions [10]. Different from the existing transportation resilience study where modified normal travel demand is adopted [11], we use a unique empirical disaster traffic dataset in Harris County, TX to help us examine the extent to which Hurricane Harvey flooding affected the network reliability and measure the network resilience throughout the network disruption and recovery phases. Such resilience characterization using empirical flood-disrupted traffic data is missing in current literature. This research will bridge this gap and provide new insights and metrics for evaluating transportation network resilience performance. Results of this research can improve our understanding of transportation resilience when facing flood disruption and facilitate stakeholders' and engineers' decision-making in traffic control during disasters.

2. Literature review

2.1. Transportation reliability

Transportation reliability is commonly studied from three perspective: connectivity reliability, capacity reliability, and travel time reliability [12–14]. Travel time reliability relates to the characterization of the travel time variation [15,16]. The U.S. Department of Transportation (USDOT) defines reliability as "the degree of certainty and predictability in travel times on the transportation system" [17]. Sterman and Schofer [18] initially computed the inverse of the standard deviation of travel time as transportation service reliability. Later, more models are developed for travel time reliability measurement. California Buffer Time Reliability model [19] uses the difference between 95th percentile travel time (i.e., planning time) and the average travel time as the buffer time. Florida DOT [20] developed the Florida Reliability model by setting an upper threshold and calculating the probability that the actual travel time does not exceed the threshold [21]. Al-Deek and Emam [21] define the link travel time reliability as the probability that the travel time at degraded capacity is less than the free-flow travel time plus a tolerance margin. Indexes such as Buffer Time Index (buffer time divided by the average travel time) [16,22,23] and Planning Time Index (dividing the 95th percentile travel time with the free-flow travel time) [16,23,24] are also developed to describe the link reliability by the time-of-the-day or day-of-the-week.

An important aspect of reliability is to determine if a trip can be completed within an expected time [21,25], such as mean degree travel time with several degrees of variation. Lo et al. [26] introduced the Within Budget Time Reliability as the probability that a trip is within the travel time budget. Similar to this definition, we translate the probability into a ratio that describes the proportion of the time that a link is underperforming, namely, the speed is lower than an acceptable level and thus cannot complete the travel within the expected time. We are not intended to replace the existing reliability definition but to present a different perspective to capture the reliability dynamics on a temporal scale.

In addition, it is critical to understand transportation system behavior in facing non-recurring congestion induced by the extreme weather, so that Metropolitan Planning Organization (MPO) planners and operations managers, and analysts can better manage the traffic in urban areas during natural disasters [27–30]. Several studies have examined the impact of link failures on transportation system performance. For example, Sullivan et al. [31] examined the impact of critical road failure on Chittenden County on transportation network robustness through a capacity-reduction approach and showed that system-wide travel time varies dramatically. Ganin et al. [32] examined the impact of small random road failure on 40 U.S. metropolitan transportation networks and showed that 5% link disruption can result in serious resilience and efficiency damages. However, previous studies all employed synthetic or adjusted normal day traffic data, which cannot fully capture the system dynamics in a disaster where flooding, congestion, and rerouting occur. This research employs the unique empirical fine-resolution traffic data during hurricane Harvey to unveil the transportation system behavior under disruptions. Moreover, we are able to examine the network reliability of a large-scale network in different phases of a disaster (stable, disruption, recovery), which has not been captured in previous studies.

2.2. Resilience measurement

Resilience has been widely studied in different fields [33,33–37], and different disciplines interpret resilience with its unique domain knowledge. Even within the same field, such as transportation, resilience is assessed from different perspectives [38]. For example, Zhang et al. [39] investigated the transportation network resilience from a topological perspective. Adjetey-Bahun et al. [40] evaluated the mass railway transportation system resilience through system efficiencies such as passenger delay and passenger load. Markolf et al. [41] discussed transportation resilience considering its interconnections with other critical infrastructure systems. Chen and Miller-Hooks [42] measures the resilience of the transportation network by calculating the expectation of the ratio between maximum demand that an origin–destination pair can satisfy after and before a disruption. Francis and Bekera [43] introduced a dynamic resilience metric by multiplying the recovery speed, the percentage of performance loss, and the percentage of the performance recovery. Therefore, no unified approach or definition of resilience can be asserted [44]. For instance, resilience characterization has been approached from different perspectives [45], including

- Vulnerability: system's susceptibility to disruption [46]
- Robustness: system's ability to absorb disturbance and remain functional [47,48]
- Reliability: the probability that a network deliver adequate functionality given a disruption [49–52]

- Recoverability: the ability of a disrupted network to recover its functionality [53]
- Redundancy: the ability of the system to undertake disruption without severely damaging the system performance [54,55]
- Rapidity: recovery with a focus on the speed to recover [56]

These metrics have been widely investigated among researchers. Berdica [57] discussed vulnerability from the perspective of reliability, robustness, resilience, and redundancy. Rather than a quantitative measure, they view vulnerability as a way of thinking. Chen et al. [58] studied transportation vulnerability by assessing the impact of network disruption on accessibility in terms of travel time or generalized travel cost increase. However, the model was only applied in a five-node network, which provides limited insights for the effective large-scale network application. Xu et al. [59] used travel alternative diversity and network spare capacity to characterize the transportation network redundancy. They can also serve as criteria for network vulnerability assessment. Recent disaster events also raised attention for transportation network vulnerability and resilience assessment [60–62].

Several studies have examined the resilience of the transportation network under disruptive events such as flood. For example, Morelli and Cunha [61] evaluated the increase in travel path length due to disruptions in different regions. They show that motorized individual transport is more vulnerable to floods, compared to walking and cycling. Papilloud and Keiler [63] assessed the direct and indirect impact of extreme floods on regional road networks based on accessibility loss. The proposed metrics take population and average shortest travel time into account when identifying highly impacted traffic. Wiśniewski et al. [64] examined the vulnerability for accessing critical facilities such as grocery stores during flooding.

Empowered by modern data collection technology, many studies also used empirical data to examine the transportation network performance in facing disruption. Esfeh et al. [65] used travel time and incident data collected in the City of Calgary to examine the spatiotemporal impact of the incident on road network vulnerability. Pan et al. [66] used the OD-grid network to assess the transportation network resilience and tested the recovery strategy using empirical GPS data. Calvert and Snelder [67] proposed the Link Performance Index for Resilience (LPIR) to assess road traffic resilience and demonstrated its application in a real motorway network. Adams et al. [68] studied freight resilience of the Hudson-Beloit corridor by examining the resilience triangle derived based on empirical truck speeds and counts. Muriel-Villegas et al. [69] used real data to investigate the interurban transportation network connectivity and vulnerability through a case study in Antioquia, Columbia. The findings of prior research have great implications for real-world transportation management. However, empirical data-driven studies are still rare, mainly due to the lack of proper methods and high-resolution data during disasters. This research complements existing literature on examining disaster impact on transportation and provides a novel robust data-driven network approach to measure the mobility reliability and resilience behavior in facing large-scale flood disruption.

In this paper, we adopt the insights from [44] and define transportation resilience as the system's ability to absorb disruptions, maintain essential structure and functionality, and timely recovery from the disruption events such as natural disasters to a new state with acceptable performance at reasonable costs. We deem that the amount of performance loss and recovery is equivalently important to the speed of such loss and recovery. Accordingly, we developed an integrated resilience measure that encapsulates vulnerability, recoverability, and rapidity for functionality recovery in Section 4.3.

2.3. Infrastructure failure characterization in resilience assessment

All resilience definitions involve the consideration of system performance in facing disruptions [70–74]. Thus, proper characterizations of the network disruption are critical in resilience assessment. In the case of the transportation network, the disruption is often modeled by modifying topological or functional attributes of road networks [75].

Topological attributes such as connectivity, emphasize the connection between infrastructures and are often studied through graph-based approaches and metrics [76]. Many studies have examined the transportation network resilience using a topological approach. For example, Dong et al. [47] examined the robustness of several road networks through random failure-based percolation. Dong et al. [77] also examined the road access to hospitals in the aftermath of a probabilistic earthquake-induced transportation network failure. Chopra et al. [78] investigated the vulnerability of the London metro network through various topology-based metrics.

The topological approach has proven to be an effective method for preliminary network resilience analysis, especially when dynamic data is limited and connectivity or critical facility access assessment is of interest. It only requires simple network topology data but provides rich information regarding the criticality of each component and how road connectivity can influence the resilience of the network. The disadvantage of the topological approach lies in the simplified binary infrastructure failure characterization. The road or intersection failures are represented with link and node removal in the simulation [77]. However, partial failure is very common in real life. For example, lane closure or traffic congestion may only compromise a fraction of the performance. In this case, dynamic functional failure can be considered.

Functional attributes mainly focus on the serviceability of the transportation network, such as travel time/speed/distance, capacity/throughput, mobility/accessibility [31,75,79]. Geng et al. [80] considered the network demand under disruption in network resilience assessment. Ganin et al. [32] examined the resilience and efficiency of multiple cities' road networks using functional measures such as travel delay. Li et al. [81] define link quality of a road at time t as the ratio of its current travel speed and maximum speed. Similarly, Hamedmoghadam et al. [82] define link quality of a road at time t as the ratio of current travel time and free-flow travel time. The road functional status is then determined by comparing the road's link quality and an acceptable performance threshold q.

The link quality approach enables the integration of both dynamic road performance and partial temporal road failure in the road failure characterization. Thus, we adopt the link quality approach in this study. More importantly, based on the aforementioned road functional status definition, a road's status can switch between functional and failure over time in dynamic transportation, such as traffic congestion or road inundation. Therefore, we further calculate the fraction of time that a link remains functional and define it as the link reliability (Eq. (2)) to evaluate the network resilience performance.

3. Methodology

The transportation network can be modeled as a graph $G(V, E, W)$ whose link attributes vary temporally. $V = \{v_1, \dots, v_n\}$ is a set of N nodes (i.e., intersections) and $E = \{e_{ij}, i, j = 1, \dots, n\}$ is the set of k links (i.e., roads) that connect node i and node j. $W = [W(t), t = 1, \dots, T]$ is a series of temporal weight matrix where $w_{ij}(t)$ represents the temporal attribute of the link e_{ij} at time t. Link quality is a dynamic feature that has been used to describe the performance of each road [81–83]. We define link quality as the ratio of travel speed (v_{ij}) at time t and the reference speed of the link (v_l). Reference speed is the "free-flow" mean speed of the link [16]. The dynamic traffic patterns make the link quality a time-variant feature as travel speed changes over time. Travel speed is used because it can directly reflect the impact of the disaster disruption on travel demand and road condition. A low travel speed (relative to the reference speed) indicates road congestion, which implies a low link quality. The link quality (v_{ij}/v_l) essentially encapsulates the extent to which the traffic on road e_{ij} is disrupted.

Ideally, link quality should equal 1, namely, vehicles expect to travel at the reference speed on all roads. However, our daily travel is compromised due to varying factors, such as increasing urbanization, traffic incidents, and disaster disruptions. We gradually develop a tolerance for travel experience degradation by adjusting our expectation or standard for link quality to a lower threshold. Depending on what level of travel speed is deemed acceptable, we can use a link quality threshold q to determine if a road is reaches expected functionality or congested at different times. We formulate this rule in Eq. (1) for determining link function status f (i.e., functional or dysfunctional).

$$f(i,j,t) = \begin{cases} 1 & v_{ij}(t)/v_l \geq q \\ 0 & v_{ij}(t)/v_l < q \end{cases} \tag{1}$$

where q is the link quality threshold that characterizes the tolerance for link performance. The quality threshold q suggests that a partially compromised link can still be considered functional if its performance is above an acceptable level. For example, for a road with a reference speed of $v_l = 60$ miles/h, $q = 0.3$ indicates that as long as the travel speed is above 18 miles/h, we consider the link is functioning. The link quality threshold q can also be interpreted as the acceptable system performance level, above which the system is considered functional. The selection of q is dependent on the city's traffic behavior and the decision-makers' goal for traffic performance.

3.1. Link reliability definition using link quality threshold

Link function status f oscillates over time. For example, travel congestion occurs during rush hours and the link function status transits from 1 to 0. While in off-peak hours, the link function will switch back to 1. This traffic pattern is commonly recognized in daily life. Such an oscillation phenomenon can also occur when a network is disrupted. For example, the flooding-induced road closure will lead to traffic rerouting, which can turn a congestion-free road into a deadlock. More importantly, the time at which a link stays functional is also critical. For instance, a link that stays congested for one hour has a better performance than a link that stays congested for four hours, in terms of its performance reliability. To capture this important temporal feature, we formulate the link reliability r_{ij} of link e_{ij} during time $\triangle t$ $(= t_n - t_m)$ as the ratio depicted in Eq. (2).

$$r_{ij}(t_m, t_n) = \frac{\sum_{t_m}^{t_n} f(i,j,t)}{\triangle t} \tag{2}$$

Link reliability of the network is represented by r in general, and it is a microscopic network performance metric that measures the proportion of time that a link's functionality stays above the link quality threshold q. If specified as r_{ij}, it indicates the reliability of the link e_{ij}. In the case of flooding, roads may be inundated and the travel speed can decrease. The resulting prolonged congestion would indicate the network quality does not meet standards over time, and thus, link reliability decreases. It is worth noting that the fluctuation range of the speed is not considered in the reliability definition. We mainly focus on determining if a road's speed/travel time meets the expectation (q) or not. Once they meet the criteria, we do not specify how much they are above or below the threshold.

3.2. Network reliability scale characterization through link reliability distribution

Spatial mapping of individual link reliability enables the identification of the critical unreliable links, whereas the holistic investigation of aggregated link reliability can reveal the network's macroscopic performance pattern. It is important to notice that roads are interconnected. So the theoretical analysis of a network should consider road correlations. However, this research uses the empirical traffic data, where impacts between roads are already captured and reflected in the observed speed. Therefore, we can examine the network performance based on aggregated link performances.

Using a hypothetical transportation network with 100 roads as an example (Fig. 2). In an off-peak hour, 90 roads are congested only in 1% of the time, 9 roads are congested in 3% of the time, and 1 road is congested in 10% of the time. As traffic increases in a rush hour, 60 roads become congested in 1% of the time, 30 links become congested in 3% of the time, and 10 links are congested in 10% of the time. The shift of link reliability slope in two scenarios reflects the network functionality change. Therefore, we investigate the distribution of link reliability across the entire network. As suggested by Jiang et al. [84], road congestion duration distribution follows a power-law distribution. Thus, we hypothesize the distribution of link reliability r across the network during a given period follows the relationship in Eq. (3):

$$p \sim (1-r)^{-\alpha} \tag{3}$$

where $-\alpha$ is the exponent that controls the slope of the distribution. $1 - r$ is the opposite of the link reliability, namely, the proportion of time that a link is congested, and p is the frequency of corresponding link congestion. In the illustrative example in Fig. 2(b), for the roads congest 1% of the time, the probability for the road holds reliability $r = 0.99 (= 1 - 0.01)$ is $p = 0.9 (= 90/100)$ in off-peak hour (i.e., blue curve) and it changes to $p = 0.6 (= 60/100)$ in peak hour (red curve).

Fig. 2(b) shows an example of α from 8:00 a.m. to 9:00 a.m. with the link quality threshold $q = 0.3$. The reliability of each link is calculated based on Eq. (2) and the opposite of reliability, $1 - r$ is then plotted in log–log scale. In this illustrative case, α equals 2.726. As suggested by Fig. 2(a), the slope reflects the network functionality. When α decreases, the fitted line becomes flat and more links become less reliable, as more values concentrate in the high $1 - r$ end, namely the low-reliability region. Similarly, the increase in α indicates more links become reliable. The change of α and r are consistent here. Therefore, we use $1-r$ in the definition and name α as the network reliability scale index. α is a macroscopic network performance metric that depicts the reliability distribution of the whole network during a given time.

3.3. Network stability characterization considering link reliability variance

We have shown that link reliability fluctuates over time due to the dynamic nature of traffic. However, such fluctuation should vary within a range to ensure the stability of the network functionality. Moreover, despite the significance of understanding the impact of link reliability reduction on network resilience, equivalently important is to consider the obvious improvement of link reliability. Because a drastic change of link performance, either improvement or degradation, can both disturb the metastability of the transportation network [5]. For example, historical data show the reliability of a selected road on a regular day varies from 0.2 to 0.5. In the case of an important sports event, the traffic worsens and the link reliability can drop to 0.1. On the other hand, when a travel restriction is implemented, fewer vehicles are on the road and the link quality can increase to 0.7. Therefore, we introduce the metric of link stability and define it as an interval, from which link behavior abnormality, both the functionality improvement and reduction, can be detected when the link reliability falls out of the defined range.

Fig. 3(a) shows a single link's (e_{ij}) dysfunction ratio ($1 - r_{ij}$) from Aug. 1 to Oct. 30, 2017 under different combinations of q and λ. We can observe that a link's dysfunction ratio normally varies within a range but fluctuates drastically during Hurricane Harvey. If we define a boundary, we can identify the network's abnormal behavior accordingly, as pointed by the yellow squares and diamonds in Fig. 3(a). When we aggregated all links' dysfunctional ratio on Aug. 16, 2017 as presented in Fig. 3(b) and fit a boundary, we can capture the stability of the network. ψ_{ij}^{l} and ψ_{ij}^{u} are the defined lower and upper bound of the dysfunction ratio of link e_{ij} based on historical baseline data. This

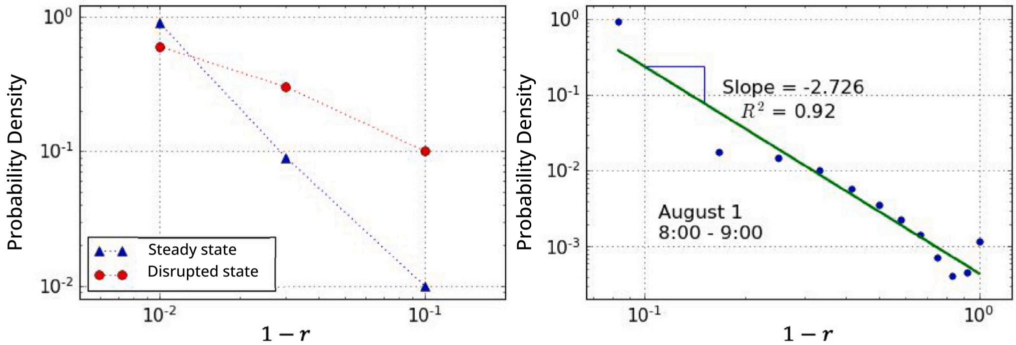

(a) Network reliability distribution characterization (b) Network reliability scale index derivation

Fig. 2. Illustrative example of network resilience scale index characterization.

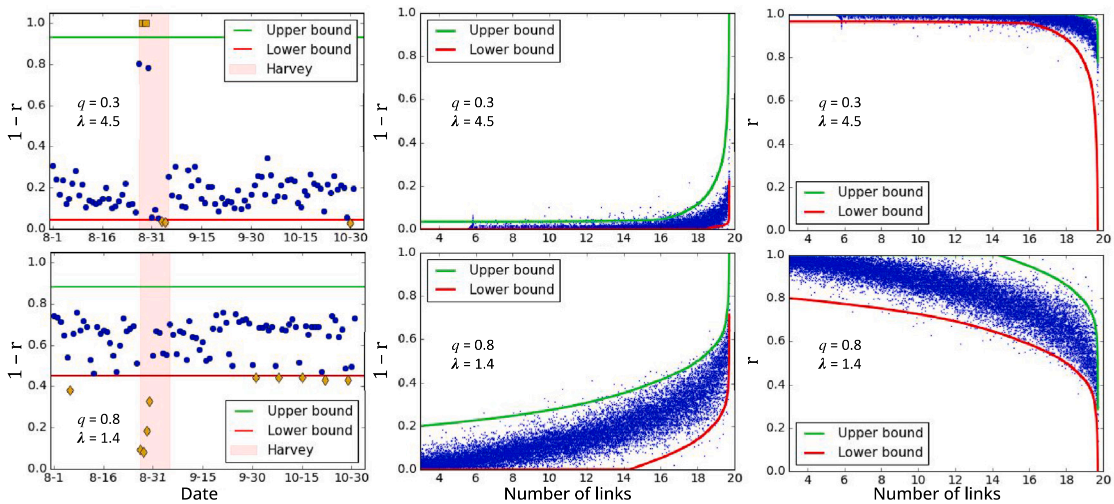

(a) Single-link temporal reliability fluctuation (b) Network-wide link reliability depicting dysfunctional links on Aug. 16th (c) Network-wide link reliability depicting functional links on Aug. 16th

Fig. 3. Single-link and network-wide reliability stability illustration, with different q and λ combinations.

boundary (i.e., curved red dash and green solid line) is the result of the concatenation of all individual link ranges.

$$\psi_{ij}^{u} = \min\{(1-r_{ij}^{b}) + \max\{\lambda(1-\overline{r^{b}}), (\lambda-1)(1-r_{ij}^{b})\}, 1\} \tag{4}$$

$$\psi_{ij}^{l} = \max\{(1-r_{ij}^{b}) - \max\{\lambda(1-\overline{r^{b}}), \frac{\lambda-1}{\lambda}(1-r_{ij}^{b})\}, 0\} \tag{5}$$

where $1-r_{ij}^{b}$ indicates the baseline dysfunction ratio of link e_{ij} and $1-\overline{r^{b}}$ is the average baseline dysfunction ratio of the whole network. λ is the tolerance factor that controls the width between the upper and lower bound.

The boundary in Eqs. (4)–(5) are empirically derived. The rationale is that we first constructed the dysfunction ratio boundary by adding or subtracting a buffer of λ times of network's average baseline value $1-\overline{r^{b}}$ to the link's baseline value $(1-r_{ij}^{b})$. In this case, the upper boundary has the possible format of $\psi_{ij}^{u} = (1-r_{ij}^{b}) + \lambda(1-\overline{r^{b}})$ and the lower boundary is $\psi_{ij}^{l} = (1-r_{ij}^{b}) - \lambda(1-\overline{r^{b}})$. However, the distribution of the dysfunction ratio is highly nonlinear at higher values. Thus, we use variations of the link's baseline value r_{ij}^{b} as the buffer. Different treatments of $\lambda-1$ and $\frac{\lambda-1}{\lambda}$ ensure we accommodate the non-linearity and only capture the extreme abnormal fluctuation behavior in both directions. In this scenario, the upper boundary has the possible format of $\psi_{ij}^{u} = \lambda(1+r_{ij}^{b})$ and the lower boundary is $\psi_{ij}^{l} = \frac{1}{\lambda}(1-r_{ij}^{b})$. Based on the value adoption for λ, different upper and lower boundary conditions can be derived. Finally, we enforce the dysfunction ratio ranges between 0 and 1.

We show that a larger λ creates a wider boundary that enables higher tolerance for heterogeneous reliability behaviors. The reason we use different λ values for different thresholds q is because, the variation of reliability fluctuation for different q values are different. We consider the network before a disaster is relatively stable. So we adjust the λ to encapsulate most of the links. In this case, we can capture how many links were behave abnormally because of the disaster.

Since the network reliability behavior is of interest, we will investigate the reliability fluctuation as shown in 3(c). The proportion of the links whose reliability falls within the define range during time $[t_m, t_n]$ is defined as the network stability s:

$$s(t_m, t_n) = \frac{1}{k}\sum_{i,j}^{n} \phi_{ij}^{t_{m,n}} \tag{6}$$

$$\phi_{ij}^{t_{m,n}} = \begin{cases} 1 & 1-\psi_{ij}^{u} \leq r_{ij}(t_m, t_n) \leq 1-\psi_{ij}^{l} \\ 0 & else \end{cases} \tag{7}$$

where $\phi_{ij}^{t_{m,n}}$ is the link stability indicator—a binary value that indicates if the reliability of link e_{ij} is within the defined range. $r_{ij}(t_m, t_n)$ then iterates through all links (k) in the network and calculates the proportion of links whose reliability value falls within the defined range during time $[t_m, t_n]$. That is to say, as long as the reliability of the link is within an expected range, we consider it as stable. Network stability s is a macroscopic performance metric that ranges from 0 to 1.

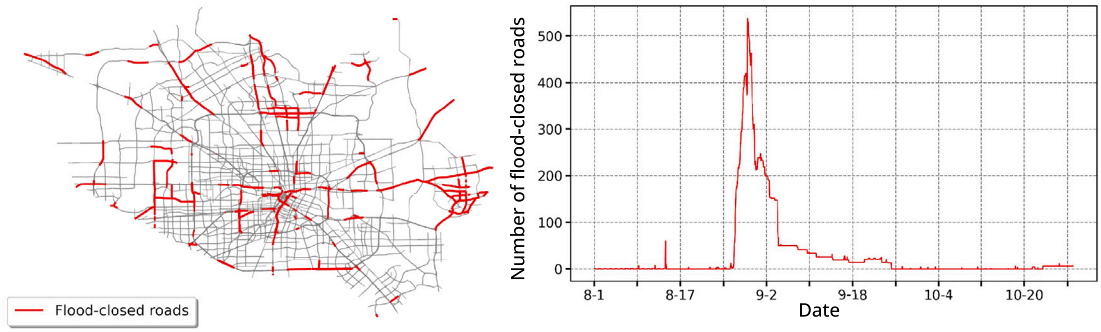

(a) Mapping of flood-closed roads

(b) Temporal development of flood-closed roads

Fig. 4. Flood-disrupted Harris County transportation network during Hurricane Harvey.

4. Road network resilience in the case of Hurricane Harvey

The proposed two network performance metrics are examined using the transportation network of Harris County, TX in the case of the 2017 Hurricane Harvey flood disruption. Hurricane Harvey stalled over Harris County, home to Houston, from August 26 to 28, and is one of the costliest extreme weather events in the United States history [85]. Fig. 4(a) maps the “closed roads” (whose travel speed reduced to 0) due to Hurricane Harvey flooding. Fig. 4(b) shows the development of such road disruption and recovery before, during, and after Hurricane Harvey. Other than the topological data, we also acquired a high-resolution traffic dataset (i.e., average traffic information every 5 min), capturing the dynamic traffic condition for the 92 days from August 1 to October 31. The traffic speed data was collected by tracking people’s mobile phone movement and its accuracy has been significantly improved over the years due to the prevalence of smartphone usage. Large-scale smartphone location-based mobility data made it possible for us to reveal the hidden empirical dynamics of the disrupted human and infrastructure system during disasters [83,86,87].

The connected network of Harris County contains 15,390 nodes and 19,712 links. Each link has both dynamic and static attributes, such as average travel speed, reference speed, binary road closure status, link coordinates, and link length. We use reference speed as the optimal travel performance, and the travel speed less than the reference speed is considered as the link quality drop. The ratio of travel speed and reference speed is defined as link quality. We propose that the road closure and partial inundation would result in traffic slowdown and rerouting that congests unflooded regions, and eventually lead to link quality drop and network resilience reduction. Depending on the link quality threshold (q) that one considers as the acceptable performance level, the road can be classified as functional or dysfunctional using Eq. (1). We use the commonly accepted definition of network resilience [88] in this paper, which describes a network’s ability to anticipate, absorb, adapt to, and recover from disruptive events. Specifically, we focus on resilience through the lens of the link reliability and stability variations in the case of flooding, and we use the Harris County road network during Hurricane Harvey as the case study.

4.1. Temporal variation of network reliability during Hurricane Harvey

Using the procedure described in Section 3.2, the network reliability scale index (α) can be derived for each hour. Repeating this procedure for every hour from August 1 to October 31, we obtained the resilience curve for the network reliability scale index, as shown in Fig. 5(a). We use the case of $q = 0.3$ as an illustration but such a resilience curve can be developed with other q values as well. We can see that the network reliability scale (α) remains stable before Harvey. However, as Hurricane Harvey approaches, an obvious drop of α can be observed (red shaded area), indicating that network resilience reduces as more links’ reliability r decreases (i.e., probability of prolonged congestion $1 - r$ increases). This can be explained by the fact that road inundation pushes the original traffic to reroute to the fewer remaining roads, which causes congestion. In addition, the inclement weather reduces the safe travel speed on roads, which further exacerbates the congestion, and therefore, the link reliability decreases. As the flood recedes, the network resilience gradually improves with roads becoming more reliable, since more roads are available for travel and road condition improves.

To better demonstrate the temporal reliability dynamics before, during, and after Hurricane Harvey flooding, we calculate the daily average reliability to remove the traffic fluctuation noise, as shown in Fig. 5(b). Considering the influence of the workday commute, we also look into the weekdays and weekends separately. We can see that link reliability during weekdays is lower than those on weekends. We can also clearly identify different stages of the resilience curve. In specific, before the onset of Harvey, the average reliability scale index α is around 2.07. As Harvey approaches, α started dropping and reaches its minimum value of 1.6 (23% of decrease) on September 1. This decline directly relates to the disruption resulting from the compound failure of flood-inundated roads and slowed traffic due to extreme weather. The reliability performance then recovers to 1.81 (13% of increase) on September 15, which can be explained by the flood water receding and the improved travel condition on the functional road. The spike in weekday curve (Fig. 5(b)) on September 4th 2017 (highlighted in the green box) is because it was Memorial day. Thus, the network’s reliability behavior on that day is closer to its weekend counterparts. The reliability performance then remains stable till September 25. This is likely the phase when dysfunctional roads (e.g., debris on roads or traffic control infrastructure malfunction) are being cleaned and properly maintained. Eventually, the reliability scale index α recovers and reaches 2.0 (10% of increase) in October and remain steady. However, the transportation system was not able to fully recover to the pre-Harvey condition, partially because the excessive debris generated after Harvey takes many months to remove and the system was not fully restored within the recovery horizon of this study [89,90]. Also, some impacts of Harvey on trips and home relocation of impacted residence continued beyond the period used in this study.

In addition to the average performance, we also examined the Inter-Quantile Range (IQR, 25th to 75th) which is indicated by the light-blue shaded area in Fig. 5(c) to show the variation of reliability of each day. A clear weekly pattern can be detected from the IQR time series. Based on the network reliability scale index (α) time series of individual weekdays and weekends, we can conclude that link variation of reliability within the day is higher during weekdays than on weekends. This is likely caused by the work commute on weekdays.

Link functionality f is determined based on link quality threshold q using Eq. (1). Meanwhile, link functionality f also defines link reliability r as in Eq. (2), whose distribution shapes the value of α. Therefore,

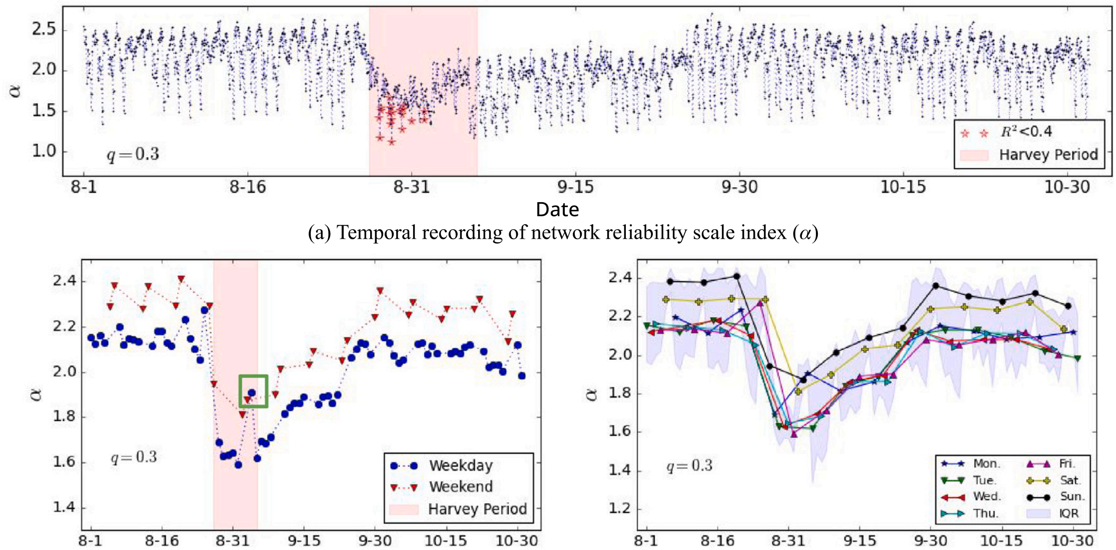

(a) Temporal recording of network reliability scale index (α)

(b) Daily average of α

(c) α by day of the week

Fig. 5. Time series of network reliability scale index α over the course of Hurricane Harvey.

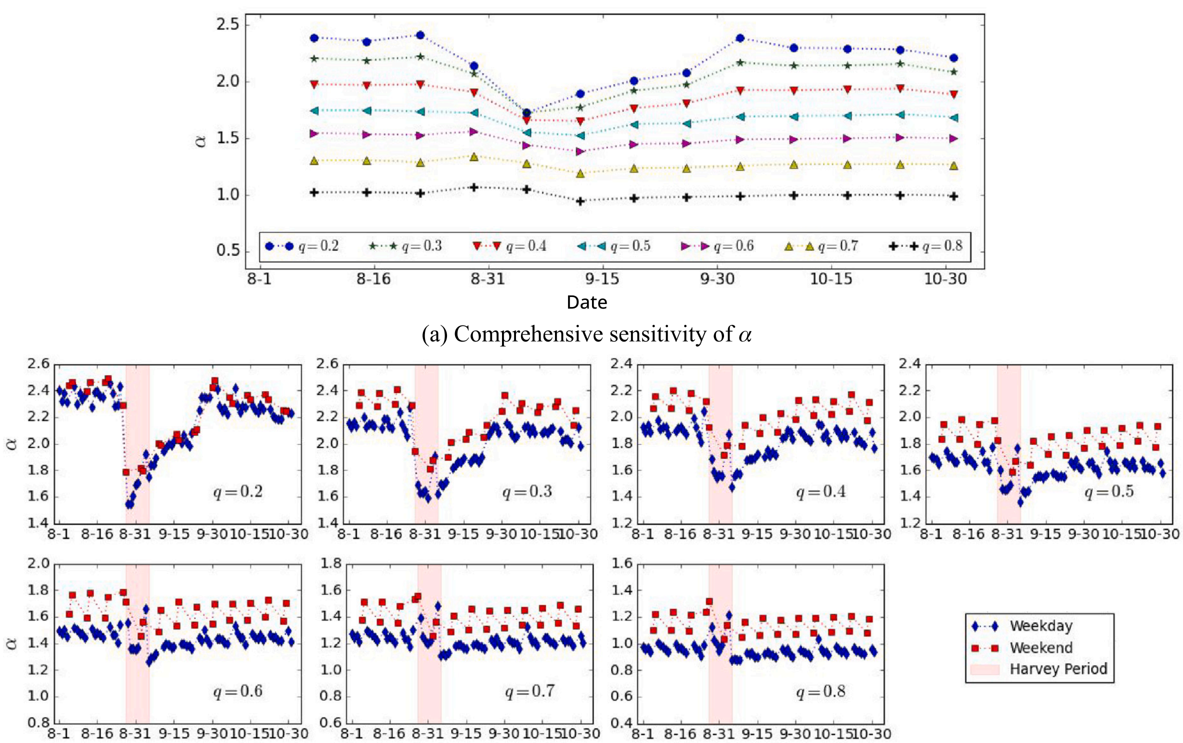

(a) Comprehensive sensitivity of α

(b) Disaggregated weekday and weekend sensitivity of α

Fig. 6. Sensitivity analysis of network reliability scale index α responding to change of link quality threshold q.

it is important to examine the sensitivity of the resilience scale index α. Fig. 6(a) shows the overall variation of α given different q values. It is worth noting that we do not consider the cases of $q = 0.1$ and $q = 0.9$ because they are extreme conditions and thus unrealistic goals for traffic regulations. Additionally, we also see abnormal behavior due to few valid data points when we attempt to fit the α based on Fig. 2.

In the case of Harris County, we can observe that as the q value increases, the "resilience triangle" become less obvious. Since the variation of network reliability scale α is more pronounced in smaller q (e.g., below 0.5) as shown in Fig. 6, it indicates that Harris County's traffic fluctuation mainly oscillates at the lower level and is thus better captured by smaller q. This is unique to each city's traffic condition. Harris County is the home to Houston, a large metropolitan area, so the link quality is generally lower. A high link quality threshold q may not be able to capture the lower level travel speed change. For example, on a road with a reference speed of 60 miles/h, the pre-Harvey average travel speed can drop from 30 miles/h to 18 miles/h during Harvey. If $q = 0.4$ is considered, the functional status of this road changes from 1 (functional) to 0 (dysfunctional) according to Eq. (1), which consequently affects the derivation of reliability r and reliability scale

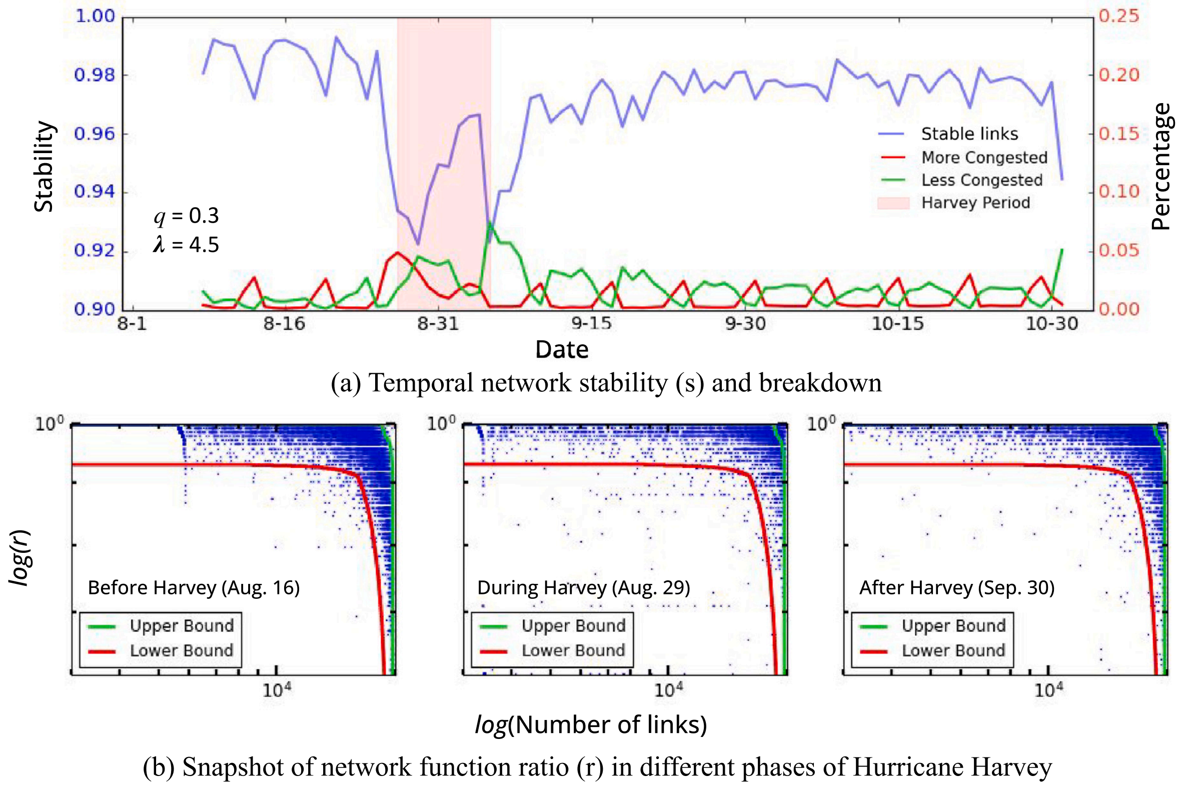

Fig. 7. Network reliability stability fluctuation throughout Hurricane Harvey.

α as in Eqs. (2) and (3). However, if a larger q is employed (a higher standard of what travel speed is considered as the acceptable travel performance), such as $q = 0.6$, the road's function status f before and during Harvey are all considered unacceptable. Thus, the reliability r remains the same, and consequently, the reliability scale index α does not change, which explains why the variation of reliability scale index α before and during Harvey becomes smaller in high q values in this study. Therefore, the selection of q needs to be based on the city's traffic and the decision-maker's goal for traffic reliability control. A less congested city may require a larger link quality threshold q for proper reliability characterization and resilience assessment. Additionally, the α value for larger q is low from the beginning (e.g., bottom lines in Fig. 6(a)). That means fewer links satisfy the high-quality requirement overall. Even if they become dysfunctional due to the flood disruption, the change to the already-low reliability is small.

Moreover, a close examination of network reliability scale α in Fig. 6(b) suggests that network reliability increases during Harvey, despite by a smaller margin. This is because, although the inundation results in road closure and speed drop on certain roads, the travel demand decreased on a small fraction of functional roads, which in turn enables a higher travel speed that led to the small reliability increase. It soon decreases when travel demand climbs back when rain stops and flood recedes.

4.2. Hurricane Harvey flooding-disturbed network stability

In a steady-state, link reliability acts in stable patterns. For example, some major roads are always congested during the weekday rush hours. In the face of disruption, such a pattern can be disrupted as the congestion will be exacerbated (e.g., travel rerouting) or alleviated (e.g., travel demand reduction). When both changes exceed a tolerable range, the change will perturb the network and result in abnormal traffic behavior. The network stability s metric proposed in Section 3.3 enables us to capture the flood-disrupted network reliability variation. We use the first two weeks of August as the baseline to derive the upper ($\psi^{l}_{i,j}$) and lower ($\psi^{l}_{i,j}$) bound of the reliability fluctuation range (Eq. (7)). We present the resilience performance of network stability throughout Hurricane Harvey in Fig. 7 in the case of $q = 0.3, \lambda = 4.5$.

We observe a clear disruption in network stability pattern during Hurricane Harvey (the fourth week of August to the second week of September in 2017) in Fig. 7. The network stability first decreases as Hurricane Harvey approaches and then drops to the minimum. The solid blue curve in Fig. 7(a) describes the fraction of roads whose reliability stay within the Eq. (7) defined range. Fig. 7(b) visualizes the stability characterization in log-scale. We can see that the reliability (r) of most roads is within the stability boundary before Hurricane Harvey. The stable pattern is disrupted during Hurricane Harvey as many links (i.e., blue dots) fall out of the stability boundary. As Harris County recovers after Hurricane Harvey, most outliers return to a stable state.

We further decompose the roads with abnormal reliability behavior. As shown in Fig. 7(a), the red curve represents the proportion of links that become more congested, and the green solid curve depicts those links that become less congested. We can see that as Hurricane Harvey approaches, there is an increase in both congested (due to inundation-induced road closure) and alleviated roads (due to reduced travel demand). As Hurricane Harvey rainfall diminishes, more people start to travel but the flood has not entirely receded. Thus, the number of less-congested roads decreases and the number of more-congested roads continues to grow, till flood inundation and debris cleaning take into effect.

Network reliability shows different patterns on weekdays and weekends (Fig. 5). Hence, we examine the network stability on weekdays and weekends separately. Also, Fig. 3 has shown that the value of tolerance factor λ can affect the width of the stability range. Therefore, we derive an optimal λ for each q. We assume that the network is stable before Hurricane Harvey. Therefore, we adjusted λ for each q to make sure 99% of links are within the stability range, namely, the smallest λ that enables the stability range to encapsulate 99% of the

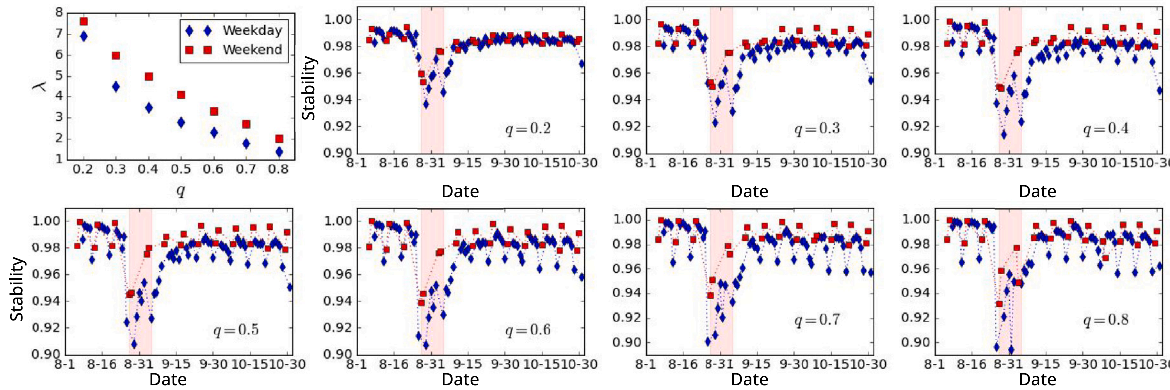

Fig. 8. Network reliability stability for weekday and weekend under different λ and q.

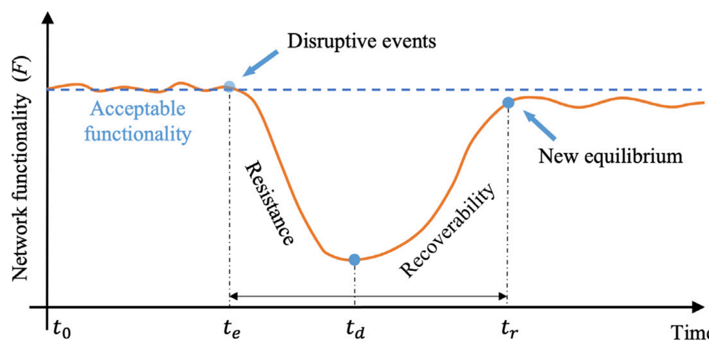

Fig. 9. Illustrative diagram of the network resilience attributes.

links in baseline condition. Fig. 8 delineates the non-linear relationship between q and λ in weekday and weekend and shows the network stability characterization for weekdays and weekends at different stages of Hurricane Harvey. We can conclude that as q increases, the required λ decreases. Just like the network reliability pattern in Fig. 6, the stability of the reliability drops as the Harvey approaches and recovers when the flood recedes. A similar "resilience triangle" is captured by the stability curve. Additionally, we observe that as the q increases, the stability value during Harvey decreases as well. That suggests the highly functional roads prior to Harvey are sensitive to flood disruption. Also, a spike appears during Harvey because the flood not only inundates the road but also reduces travel demand, which leads to improved performance on certain roads. It falls back when flood recedes and travel demand picks up.

4.3. Transportation network resilience characterization

Temporal examination of network reliability scale index (α) and reliability stability (s) in Figs. 6 and 8 both show an obvious "resilience triangle" pattern that the network functionality first decreases in a case of disruption and then recover over time as shown in Fig. 9. Adams et al. [68] used an R4 framework to measure the resilience of the freight system. In this study, we propose a comprehensive metric R [43,91] to capture the transportation system resilience, as delineated in Eq. (8). In this definition, we put an emphasis on the recovery part of the resilience process and measure the rapidity and capability of the system "bounce back" to the new equilibrium from the disrupted state. Faster recovery of the majority of lost capacity indicates a more resilient system.

$$R = \frac{F_{t_d}}{F_{t_e}} \times \frac{F_{t_r} - F_{t_d}}{F_{t_e} - F_{t_d}} \times \frac{F_{t_r} - F_{t_d}}{t_r - t_d} \tag{8}$$

The proposed resilience metric contains three components. First, the remaining performance ratio F_{t_d}/F_{t_e} captures the capacity of system stave off the disruption impact [91] or to absorb disruptions before recovery actions [43]. A larger ratio indicates less functionality loss, and thus, less vulnerable to network disruption. Second, $(F_{t_r} - F_{t_d})/(F_{t_e} - F_{t_d})$ describes the amount of system functionality recovered compared to the total functionality disruption. Hence, it shows the recoverability of the system or the adaptive capacity of the system to recover the lost functionality [43]. Third, the ratio, $(F_{t_r} - F_{t_d})/(t_r - t_d)$, represents the rapidity of the functionality restoration. This ratio (i.e., recovered functionality and time cost) describes how quickly the system reaches the new equilibrium from the lowest performance level. A larger ratio indicates a speedy recovery of the system, and thus, higher resilience.

Using different resilience metrics introduced above, we examine the Harris County transportation network resilience in the case of Hurricane Harvey flooding-induced disruption, including both road inundation and congestion. Based on the reliability and stability characterization presented in Figs. 5 and 8, we consider time of disruption occurrence (t_e) is on August 24 (i.e. a day before Hurricane Harvey landed [92]). We propose that people's travel behavior has started to change in anticipation of Hurricane Harvey. t_d is the day when network functionality drops to the minimum, and t_n is the day that the system functionality reaches its maximum within the time horizon of this dataset. With more data, a more holistic inspection of the post-Harvey recovery can be achieved and a new equilibrium date may be obtained in the future. To eliminate the daily fluctuation, we use the two-week average of network performance (e.g., network resilience scale and stability) as the steady-state baseline. We investigate the weekday and weekends separately in resilience measurement.

Fig. 10 shows how different resilience attributes change in terms of network reliability and stability based on different selections of q. For network reliability scale α during weekdays Fig. 10(a), we can see that using a large q as the functional threshold, the network shows a higher

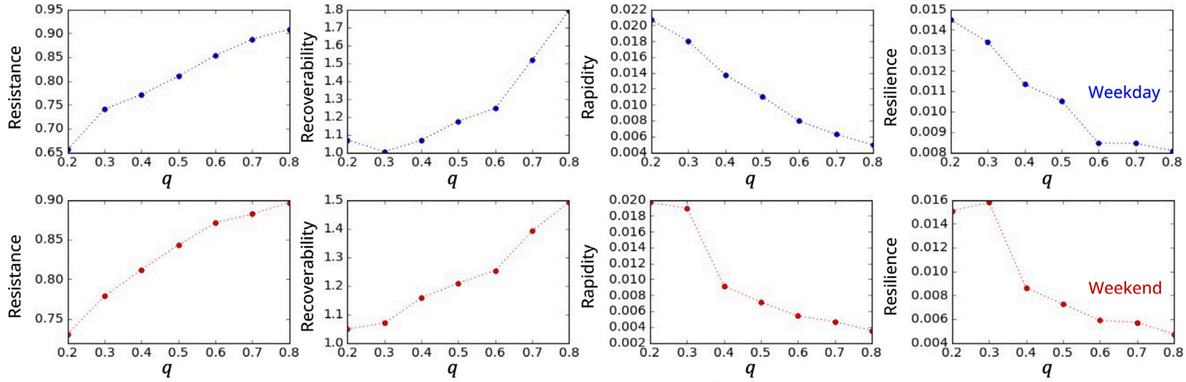

(a) Resilience characterization through network resilience scale index (α)

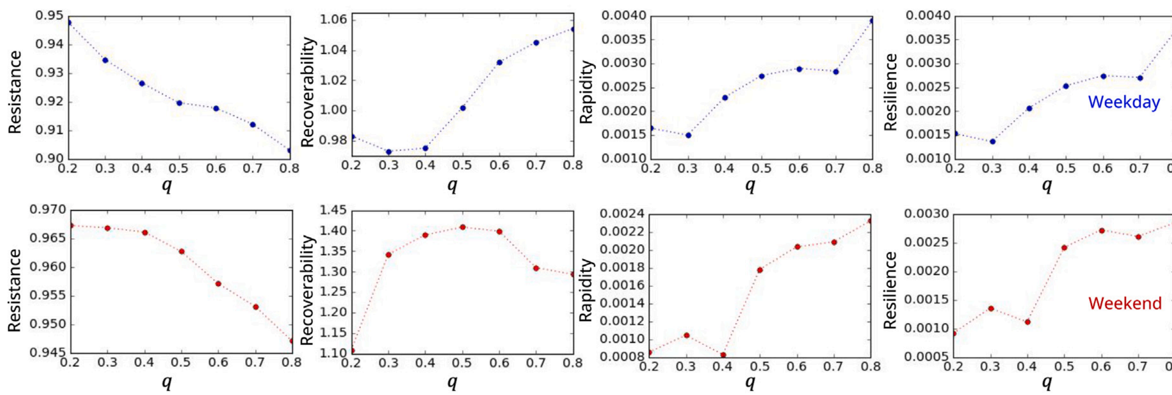

(b) Resilience characterization through network stability (s)

Fig. 10. Network resilience summary through the lens of temporal network reliability scale index (α) and network stability (s).

resistance. This means that when a larger q is selected, the low-level link quality change will not be reflected in α. For instance, considering q = 0.7 for a road of reference speed of 60 mile/h, speed drop from 40 mile/h to 30 mile/h will not affect α as the link is considered dysfunctional in both cases. The increasing recoverability indicates that most of the functionality can be restored for the high quality roads. However, the decreasing rapidity suggests that recovery for high quality roads is slow and takes longer time to recover. Overall, the network is more resilient when a low functionality standard (i.e., smaller q) is considered.

Fig. 10(b) shows that stability resistance decreases on both weekdays and weekends when strict performance requirements (i.e., large q) is considered. One plausible explanation is that high-quality roads are more sensitive to flood disruption (e.g., inundation and rerouting-induced congestion). The increasing recoverability and rapidity suggest high-quality roads recover better and faster. This is because a wider stability range is considered for large q, and thus, it is easier for link reliability to return inside of the range. Although the rapidity increase, the increase is very small and mainly because of a small number of links' stability change. In all, the resilience of the network reliability stability increases for large q. It is worth mentioning that we are not intended to compare resilience for different q. After all, the selection of q should be based on the city's traffic and decision-maker's goal for traffic performance. We comprehensively present the network behavior under different q here to engineers and stakeholders and aim to facilitate traffic control and emergency management decision-making.

5. Discussion

According to the sensitivity analysis of reliability scale index α given different link quality threshold q values (Fig. 6), a proper definition of acceptable travel quality is essential in a disaster-disrupted traffic resilience analysis. An impractical acceptable travel performance standard would lead to a false estimation of urban traffic resilience since inaccurate reliability reduction and recovery would be captured. In addition, such a definition of link quality threshold q values should be based on the perspectives of both the traffic operators and road users. Otherwise, the incongruence can create a gap between desired traveler experience level and the targeted infrastructure performance goal, which would be further exacerbated in the case of a disruptive event and exacerbate the mobility hardship experienced during disasters, and potentially worsen the transportation mobility and accessibility disparity [93,94].

Besides, a uniform link quality threshold q is used across the network to determine the functionality of the road. However, based on the classification of each road, people may have various service expectations for different roads. For example, a critical path to a critical facility is expected to maintain higher link quality than a regular local road. For example, a survey can be designed to collect people's travel expectations and different link quality thresholds can be applied to the corresponding roads to evaluate the link reliability. In doing so, a traveler-centric road network resilience pattern can be derived.

Furthermore, a customized reliability range is introduced in this study to detect abnormal reliability fluctuation. However, other boundary conditions can be derived with more empirical data in the future. Similarly, the maximum–minimum or mean–variance approach can be also used. Besides, a professional-defined acceptable reliability range can be adopted in practice to better monitor the transportation network performance. Other than the reliability range, the fluctuation range of the speed oscillation can also be considered when characterizing the link quality and reliability.

Moreover, currently, we use the timestamp t_d when system performance reaches the minimum value as the critical point for disruption and recovery. In reality, however, there might exist a time period when the system performance remains stable for the emergency response to be collected and take effect, as suggested in [91]. The length of this time can be used as a metric or indicator for evaluating emergency response efficiency. On the other hand, the system may not require full recovery to provide essential service. Therefore, a fraction (e.g., 85%) of the performance recovery can be used as the signal of new equilibrium to re-assess different metrics in Eq. (8).

Finally, diverse critical infrastructures are coupled together and depend on each other, including transportation, water/food supply, communications, fuel, financial transactions, and power stations. These complex relationships are characterized by multiple connections between infrastructures, forming a network of networks [95–98]. The links create an intricate web that, depending on the characteristics of its linkages, can transmit shocks throughout broad swaths of an economy and across multiple infrastructures. Thus, it is vital to extend our approach to a network of infrastructure systems, enabling us to measure the reliability and stability of complex infrastructure services as a whole.

6. Conclusion

The new characterization of transportation network resilience from the perspective of link reliability and stability advances the understanding of infrastructure network resilience to extreme events beyond topology-based measures. The incorporation of link reliability broadens the conventional binary link failure characterization by considering the partial function loss results from service quality reduction. And the notion of link quality is adopted to integrate stakeholders' traffic operation goals for travel speed. We used the Harris County transportation network during Hurricane Harvey as the case study. Based on the empirical traffic data during disasters, we developed a scale index to describe the network-wide reliability distribution shift when facing flood disruptions over time. We also introduced a tolerance-driven boundary condition to detect anomalies in network reliability fluctuation. We showed that network reliability and stability can well capture the network performance evolution. A non-linear relation between the tolerance factor λ and link quality threshold q was discovered and the temporal network stability pattern was extracted. We proposed a comprehensive resilience measure that encapsulates the network resistance, recoverability, and rapidity in facing flood disruption and tested it on the Harris County transportation network.

The case shows that each of the proposed metrics provides a unique property for the quantification of resilience based on network dynamics and functionality. The promising results of this paper shed light on the relationship between reliability, stability, and resilience and provide a new perspective for assessing the dynamic transportation network resilience during floods. The improved understanding of linkages between link attributes and network behavior provides traffic managers a tool to more comprehensively examine network resilience through collective road performance monitoring in the face of disaster disruptions.

The proposed metrics are very generic and can be adopted in other cities and events. The proposed study uses high-resolution traffic data which contains the travel speed on the major roads of Harris County, Texas every 5 min. Similar empirical traffic data are available for different cities and events. Researchers can acquire the data by developing research partnerships with mobility companies or directly requesting it from the local Department of Transportation. The proposed methods can also be used to assess the impact of future hazards. With massive historical and real-time traffic data, advanced deep learning techniques, and accurate weather forecasts, traffic engineers can now predict the traffic pattern based on the historical traffic behavior given the weather forecast. With predicted traffic on each road, emergency managers can then apply the proposed reliability method to evaluate the extent to which the incoming disaster affects the transportation system performance and derive targeted strategies to enhance transportation resilience. Also, we can adjust the traffic speed based on the flood depth and evaluate how transportation reliability and resilience change in different flood scenarios to facilitate stakeholders' decision-making on infrastructure protection.

Moreover, the proposed method is not limited to transportation networks. Other natural, physical, social, and engineered networks with time-variant functionality states and properties could also be examined and characterized using the proposed metrics. For example, excessive viewing requests for special events or breaking news incidents can stress the telecommunication network and results in jammed content streaming. Similarly, the surging demand for electricity can overload the power network. Both infrastructure networks can also be disrupted by man-made attacks or extreme weather events, from which the infrastructure functionality is compromised and the network resilience is tested. In these cases, link quality can be measured by the information packet passed through a telecommunication link or electricity passed through the power line. By measuring the proportion of time that the infrastructure component is delivering an acceptable level of service, we can measure the network resilience in providing reliable and stable infrastructure service during disruptions.

CRediT authorship contribution statement

Shangjia Dong: Writing – original draft, Writing – review & editing, Visualization, Software, Methodology, Formal analysis, Supervision, Project administration, Funding acquisition, Conceptualization. **Xinyu Gao:** Writing – review & editing, Visualization, Software, Methodology, Formal analysis, Conceptualization. **Ali Mostafavi:** Writing – review & editing, Formal analysis, Supervision, Project administration, Funding acquisition, Conceptualization. **Jianxi Gao:** Writing – review & editing, Methodology, Formal analysis, Supervision, Project administration, Funding acquisition, Conceptualization. **Utkarsh Gangwal:** Writing – review & editing, Visualization, Software, Formal analysis.

Declaration of competing interest

The authors declare the following financial interests/personal relationships which may be considered as potential competing interests: Shangjia Dong reports financial support was provided by University of Delaware Research Foundation. Ali Mostafavi reports financial support was provided by National Science Foundation. Jianxi Gao reports financial support was provided by National Science Foundation. Jianxi Gao reports financial support was provided by Rensselaer-IBM AI Research Collaboration.

Data availability

The authors do not have permission to share data.

Acknowledgments

The authors would like to acknowledge funding support from the US National Science Foundation under award #1832662. J.G acknowledges the support of the US National Science Foundation under grant #2047488, the Rensselaer-IBM AI Research Collaboration. S.D. acknowledges the support from the University of Delaware Research Foundation, United States of America under Grant 21A00986. We also thank INRIX for providing the data. Any opinions, conclusion, and recommendations expressed in this research are those of the authors and do not necessarily reflect the view of the funding agencies. The authors would also like to thank the Editor and the anonymous reviewers for their constructive comments and valuable insights to improve the quality of the article.

References

[1] Boakye Jessica, Guidotti Roberto, Gardoni Paolo, Murphy Colleen. The role of transportation infrastructure on the impact of natural hazards on communities. Reliab Eng Syst Saf 2022;219:108184.

[2] Dong Shangjia, Wang Haizhong, Mostafizi Alireza, Song Xuan. A network-of-networks percolation analysis of cascading failures in spatially co-located road-sewer infrastructure networks. Phys. A 2020;538:122971.

[3] Wang Weiping, Yang Saini, Stanley H Eugene, Gao Jianxi. Local floods induce large-scale abrupt failures of road networks. Nature Commun 2019;10(1):1–11.

[4] Gao Jianxi, Buldyrev Sergey V, Stanley H Eugene, Havlin Shlomo. Networks formed from interdependent networks. Nat Phys 2012;8(1):40–8.

[5] Zeng Guanwen, Gao Jianxi, Shekhtman Louis, Guo Shengmin, Lv Weifeng, Wu Jianjun, Liu Hao, Levy Orr, Li Daqing, Gao Ziyou, et al. Multiple metastable network states in urban traffic. Proc Natl Acad Sci 2020;117(30):17528–34.

[6] Dong Shangjia, Esmalian Amir, Farahmand Hamed, Mostafavi Ali. An integrated physical-social analysis of disrupted access to critical facilities and community service-loss tolerance in urban flooding. Comput Environ Urban Syst 2020;80:101443.

[7] Gangwal Utkarsh, Dong Shangjia. Critical facility accessibility rapid failure early-warning detection and redundancy mapping in urban flooding. Reliab Eng Syst Saf 2022;224:108555.

[8] Farahmand Hamed, Dong Shangjia, Mostafavi Ali. Network analysis and characterization of vulnerability in flood control infrastructure for system-level risk reduction. Comput Environ Urban Syst 2021;89:101663.

[9] Zeng Weiliang, Miwa Tomio, Morikawa Takayuki. Prediction of vehicle CO2 emission and its application to eco-routing navigation. Transp Res C 2016;68:194–214.

[10] Pimm Stuart L, Donohue Ian, Montoya José M, Loreau Michel. Measuring resilience is essential to understand it. Nature Sustain 2019;2(10):895–7.

[11] Yu Dapeng, Yin Jie, Wilby Robert L, Lane Stuart N, Aerts Jeroen CJH, Lin Ning, Liu Min, Yuan Hongyong, Chen Jianguo, Prudhomme Christel, et al. Disruption of emergency response to vulnerable populations during floods. Nature Sustain 2020;3(9):728–36.

[12] Chen Anthony, Yang Hai, Lo Hong K, Tang Wilson H. Capacity reliability of a road network: an assessment methodology and numerical results. Transp Res B 2002;36(3):225–52.

[13] Gore Ninad, Pulugurtha Srinivas S, Arkatkar Shriniwas, Joshi Gaurang. Congestion index and reliability-based freeway level of service. J Transp Eng A: Syst 2021;147(6):04021027.

[14] Pennetti Cody A, Fontaine Michael D, Jun Jungwook, Lambert James H. Evaluating capacity of transportation operations with highway travel time reliability. Reliab Eng Syst Saf 2020;204:107126.

[15] Cambridge Systematics. Traffic congestion and reliability: Trends and advanced strategies for congestion mitigation. Technical report, United States: Federal Highway Administration; 2005.

[16] Kodupuganti Swapneel R, Pulugurtha Srinivas S. Link-level travel time measures-based level of service thresholds by the posted speed limit. Transp Res Interdiscip Perspect 2019;3:100068.

[17] Culotta Kalle, Fang Vincent, Habtemichael Filmon, Pape Douglas. Does travel time reliability matter? Technical report, United States: Federal Highway Administration. Office of Operations; 2019.

[18] Sterman Brian P, Schofer Joseph L. Factors affecting reliability of urban bus services. Transp Eng J ASCE 1976;102(1):147–59.

[19] Chen Chao, Skabardonis Alexander, Varaiya Pravin. Travel-time reliability as a measure of service. Transp Res Rec 2003;1855(1):74–9.

[20] Florida DOT. The florida reliability method in florida's mobility performance measures program. Florida Dep Transp 2000.

[21] Al-Deek Haitham, Emam Emam B. New methodology for estimating reliability in transportation networks with degraded link capacities. J Intel Transp Syst 2006;10(3):117–29.

[22] Lomax Tim, Turner Shawn, Margiotta Richard. Monitoring urban roadways in 2000: Using archived operations data for reliability and mobility measurement. Pub. no. FHWA-OP-02-029, Washington: Federal Highway Administration; 2004, 2001.

[23] Lyman Kate, Bertini Robert L. Using travel time reliability measures to improve regional transportation planning and operations. Transp Res Rec 2008;2046(1):1–10.

[24] Sisiopiku Virginia P, Islam MDS. A freeway travel time reliability study. Int J Eng Res Dev 2012;3(10):83–101.

[25] Yeh Cheng-Ta, Lin Yi-Kuei, Yeng Louis Cheng-Lu, Huang Pei-Tzu. Reliability evaluation of a multistate railway transportation network from the perspective of a travel agent. Reliab Eng Syst Saf 2021;214:107757.

[26] Lo Hong K, Luo XW, Siu Barbara WY. Degradable transport network: travel time budget of travelers with heterogeneous risk aversion. Transp Res B 2006;40(9):792–806.

[27] Dowling R, Parks K, Nevers B, Josselyn J, Gayle S. Incorporating reliability into the congestion management process: A primer. Washington, DC: USDOT; 2015.

[28] Chen Dingjun, Fang Xufeng, Li Yao, Ni Shaoquan, Zhang Qingpeng, Sang Chin Kwai. Three-level multimodal transportation network for cross-regional emergency resources dispatch under demand and route reliability. Reliab Eng Syst Saf 2022;222:108461.

[29] Lu Qing-Chang, Zhang Lei, Xu Peng-Cheng, Cui Xin, Li Jing. Modeling network vulnerability of urban rail transit under cascading failures: A coupled map lattices approach. Reliab Eng Syst Saf 2022;221:108320.

[30] Zhang Jianhua, Wang Ziqi, Wang Shuliang, Shao Wenchao, Zhao Xun, Liu Weizhi. Vulnerability assessments of weighted urban rail transit networks with integrated coupled map lattices. Reliab Eng Syst Saf 2021;214:107707.

[31] Sullivan James L, Novak David C, Aultman-Hall Lisa, Scott David M. Identifying critical road segments and measuring system-wide robustness in transportation networks with isolating links: A link-based capacity-reduction approach. Transp Res A 2010;44(5):323–36.

[32] Ganin Alexander A, Kitsak Maksim, Marchese Dayton, Keisler Jeffrey M, Seager Thomas, Linkov Igor. Resilience and efficiency in transportation networks. Sci Adv 2017;3(12):e1701079.

[33] Wang Nanxi, Yuen Kum Fai. Resilience assessment of waterway transportation systems: Combining system performance and recovery cost. Reliab Eng Syst Saf 2022;226:108673.

[34] Yin Jiateng, Ren Xianliang, Liu Ronghui, Tang Tao, Su Shuai. Quantitative analysis for resilience-based urban rail systems: A hybrid knowledge-based and data-driven approach. Reliab Eng Syst Saf 2022;219:108183.

[35] Rachunok Benjamin, Nateghi Roshanak. The sensitivity of electric power infrastructure resilience to the spatial distribution of disaster impacts. Reliab Eng Syst Saf 2020;193:106658.

[36] Guidotti Roberto, Gardoni Paolo, Rosenheim Nathanael. Integration of physical infrastructure and social systems in communities' reliability and resilience analysis. Reliab Eng Syst Saf 2019;185:476–92.

[37] Blagojevic Nikola, Didier Max, Stojadinovic Bozidar. Quantifying component importance for disaster resilience of communities with interdependent civil infrastructure systems. Reliab Eng Syst Saf 2021;108747.

[38] Sun Wenjuan, Bocchini Paolo, Davison Brian D. Resilience metrics and measurement methods for transportation infrastructure: the state of the art. Sustain Resil Infrastruct 2020;5(3):168–99.

[39] Zhang Xiaodong, Miller-Hooks Elise, Denny Kevin. Assessing the role of network topology in transportation network resilience. J Transp Geogr 2015;46:35–45.

[40] Adjetey-Bahun Kpotissan, Birregah Babiga, Châtelet Eric, Planchet Jean-Luc. A model to quantify the resilience of mass railway transportation systems. Reliab Eng Syst Saf 2016;153:1–14.

[41] Markolf Samuel A, Hoehne Christopher, Fraser Andrew, Chester Mikhail V, Underwood B Shane. Transportation resilience to climate change and extreme weather events–beyond risk and robustness. Transp Policy 2019;74:174–86.

[42] Chen Lichun, Miller-Hooks Elise. Resilience: an indicator of recovery capability in intermodal freight transport. Transp Sci 2012;46(1):109–23.

[43] Francis Royce, Bekera Behailu. A metric and frameworks for resilience analysis of engineered and infrastructure systems. Reliab Eng Syst Saf 2014;121:90–103.

[44] Wan Chengpeng, Yang Zaili, Zhang Di, Yan Xinping, Fan Shiqi. Resilience in transportation systems: a systematic review and future directions. Transp Rev 2018;38(4):479–98.

[45] Liu Xueming, Li Daqing, Ma Manqing, Szymanski Boleslaw K, Stanley H Eugene, Gao Jianxi. Network resilience. Physics Reports 2020;971:1–108.

[46] Jenelius Erik, Petersen Tom, Mattsson Lars-Göran. Importance and exposure in road network vulnerability analysis. Transp Res A 2006;40(7):537–60.

[47] Dong Shangjia, Mostafizi Alireza, Wang Haizhong, Gao Jianxi, Li Xiaopeng. Measuring the topological robustness of transportation networks to disaster-induced failures: A percolation approach. J Infrastruct Syst 2020;26(2):04020009.

[48] Sakakibara Hiroyuki, Kajitani Yoshio, Okada Norio. Road network robustness for avoiding functional isolation in disasters. J Transp Eng 2004;130(5):560–7.

[49] Faturechi Reza, Miller-Hooks Elise. A mathematical framework for quantifying and optimizing protective actions for civil infrastructure systems. Comput-Aided Civ Infrastruct Eng 2014;29(8):572–89.

[50] Li Daqing, Zhang Qiong, Zio Enrico, Havlin Shlomo, Kang Rui. Network reliability analysis based on percolation theory. Reliab Eng Syst Saf 2015;142:556–62.

[51] Iannacone Leandro, Sharma Neetesh, Tabandeh Armin, Gardoni Paolo. Modeling time-varying reliability and resilience of deteriorating infrastructure. Reliab Eng Syst Saf 2022;217:108074.

[52] Zhang Lin, Wen Huiying, Lu Jian, Lei Da, Li Shubin, Ukkusuri Satish V. Exploring cascading reliability of multi-modal public transit network based on complex networks. Reliab Eng Syst Saf 2022;221:108367.

[53] Baroud Hiba, Barker Kash, Ramirez-Marquez Jose E, et al. Importance measures for inland waterway network resilience. Transp Res E 2014;62:55–67.

[54] Haimes Yacov Y. On the definition of resilience in systems. Risk Anal: Int J 2009;29(4):498–501.

[55] Davis Craig A, Mostafavi Ali, Wang Haizhong. Establishing characteristics to operationalize resilience for lifeline systems. Natural Hazards Rev 2018;19(4):04018014.

[56] Bruneau Michel, Chang Stephanie E, Eguchi Ronald T, Lee George C, O'Rourke Thomas D, Reinhorn Andrei M, Shinozuka Masanobu, Tierney Kathleen, Wallace William A, Von Winterfeldt Detlof. A framework to quantitatively assess and enhance the seismic resilience of communities. Earthq Spectra 2003;19(4):733–52.
[57] Berdica Katja. An introduction to road vulnerability: what has been done, is done and should be done. Transp Policy 2002;9(2):117–27.
[58] Chen Anthony, Yang Chao, Kongsomsaksakul Sirisak, Lee Ming. Network-based accessibility measures for vulnerability analysis of degradable transportation networks. Netw Spat Econ 2007;7(3):241–56.
[59] Xu Xiangdong, Chen Anthony, Jansuwan Sarawut, Yang Chao, Ryu Seungkyu. Transportation network redundancy: Complementary measures and computational methods. Transp Res B 2018;114:68–85.
[60] Kermanshah Amirhassan, Derrible Sybil. A geographical and multi-criteria vulnerability assessment of transportation networks against extreme earthquakes. Reliab Eng Syst Saf 2016;153:39–49.
[61] Morelli André Borgato, Cunha André Luiz. Measuring urban road network vulnerability to extreme events: an application for urban floods. Transp Res D 2021;93:102770.
[62] Zhang Mingyuan, Yang Xiangjie, Zhang Juan, Li Gang. Post-earthquake resilience optimization of a rural "road-bridge" transportation network system. Reliab Eng Syst Saf 2022;225:108570.
[63] Papilloud Tsolmongerel, Keiler Margreth. Vulnerability patterns of road network to extreme floods based on accessibility measures. Transp Res D 2021;100:103045.
[64] Wiśniewski Szymon, Borowska-Stefańska Marta, Kowalski Michał, Sapińska Paulina. Vulnerability of the accessibility to grocery shopping in the event of flooding. Transp Res D 2020;87:102510.
[65] Esfeh Mohammad Ansari, Kattan Lina, Lam William HK, Salari Mostafa, Esfe Reza Ansari. Road network vulnerability analysis considering the probability and consequence of disruptive events: A spatiotemporal incident impact approach. Transp Res C 2022;136:103549.
[66] Pan Xing, Dang Yuheng, Wang Huixiong, Hong Dongpao, Li Yuehong, Deng Hongxu. Resilience model and recovery strategy of transportation network based on travel OD-grid analysis. Reliab Eng Syst Saf 2022;223:108483.
[67] Calvert Simeon C, Snelder Maaike. A methodology for road traffic resilience analysis and review of related concepts. Transp A 2018;14(1–2):130–54.
[68] Adams Teresa M, Bekkem Kaushik R, Toledo-Durán Edwin J. Freight resilience measures. J Transp Eng 2012;138(11):1403–9.
[69] Muriel-Villegas Juan E, Alvarez-Uribe Karla C, Patiño-Rodríguez Carmen E, Villegas Juan G. Analysis of transportation networks subject to natural hazards–Insights from a Colombian case. Reliab Eng Syst Saf 2016;152:151–65.
[70] Fan Dongming, Sun Bo, Dui Hongyan, Zhong Jilong, Wang Ziyao, Ren Yi, Wang Zili. A modified connectivity link addition strategy to improve the resilience of multiplex networks against attacks. Reliab Eng Syst Saf 2022;221:108294.
[71] Liu Wei, Song Zhaoyang. Review of studies on the resilience of urban critical infrastructure networks. Reliab Eng Syst Saf 2020;193:106617.
[72] Poulin Craig, Kane Michael B. Infrastructure resilience curves: Performance measures and summary metrics. Reliab Eng Syst Saf 2021;216:107926.
[73] Han Lin, Zhao Xudong, Chen Zhilong, Gong Huadong, Hou Benwei. Assessing resilience of urban lifeline networks to intentional attacks. Reliab Eng Syst Saf 2021;207:107346.
[74] Yarveisy Rioshar, Gao Chuan, Khan Faisal. A simple yet robust resilience assessment metrics. Reliab Eng Syst Saf 2020;197:106810.
[75] Faturechi Reza, Miller-Hooks Elise. Measuring the performance of transportation infrastructure systems in disasters: A comprehensive review. J Infrastruct Syst 2015;21(1):04014025.
[76] Huang Wencheng, Zhou Bowen, Yu Yaocheng, Yin Dezhi. Vulnerability analysis of road network for dangerous goods transportation considering intentional attack: Based on cellular automata. Reliab Eng Syst Saf 2021;214:107779.
[77] Dong Shangjia, Wang Haizhong, Mostafavi Ali, Gao Jianxi. Robust component: a robustness measure that incorporates access to critical facilities under disruptions. J R Soc Interface 2019;16(157):20190149.
[78] Chopra Shauhrat S, Dillon Trent, Bilec Melissa M, Khanna Vikas. A network-based framework for assessing infrastructure resilience: a case study of the London metro system. J R Soc Interface 2016;13(118):20160113.
[79] Murray-Tuite Pamela M, Mahmassani Hani S. Methodology for determining vulnerable links in a transportation network. Transp Res Rec 2004;1882(1):88–96.
[80] Geng Sunyue, Liu Sifeng, Fang Zhigeng. A demand-based framework for resilience assessment of multistate networks under disruptions. Reliab Eng Syst Saf 2022;222:108423.
[81] Li Daqing, Fu Bowen, Wang Yunpeng, Lu Guangquan, Berezin Yehiel, Stanley H Eugene, Havlin Shlomo. Percolation transition in dynamical traffic network with evolving critical bottlenecks. Proc Natl Acad Sci 2015;112(3):669–72.
[82] Hamedmoghadam Homayoun, Jalili Mahdi, Vu Hai L, Stone Lewi. Percolation of heterogeneous flows uncovers the bottlenecks of infrastructure networks. Nature Commun 2021;12(1):1–10.
[83] Dong Shangjia, Gao Xinyu, Mostafavi Ali, Gao Jianxi. Modest flooding can trigger catastrophic road network collapse due to compound failure. Commun Earth Environ 2022;3(23).
[84] Jiang Yinan, Kang Rui, Li Daqing, Guo Shengmin, Havlin Shlomo. Spatio-temporal propagation of traffic jams in urban traffic networks. 2017, arXiv preprint arXiv:1705.08269.
[85] Van Oldenborgh Geert Jan, Van Der Wiel Karin, Sebastian Antonia, Singh Roop, Arrighi Julie, Otto Friederike, Haustein Karsten, Li Sihan, Vecchi Gabriel, Cullen Heidi. Attribution of extreme rainfall from Hurricane harvey, august 2017. Environ Res Lett 2017;12(12):124009.
[86] Yabe Takahiro, Jones Nicholas KW, Rao P Suresh C, Gonzalez Marta C, Ukkusuri Satish V. Mobile phone location data for disasters: A review from natural hazards and epidemics. Comput Environ Urban Syst 2022;94:101777.
[87] Hong Boyeong, Bonczak Bartosz J, Gupta Arpit, Kontokosta Constantine E. Measuring inequality in community resilience to natural disasters using large-scale mobility data. Nature Commun 2021;12(1):1–9.
[88] NIAC. National infrastructure advisory council, critical infrastructure resilience: Final report and recommendations. 2009, see https://www.cisa.gov/publication/niac-critical-infrastructure-resilience-final-report, accessed at 10/26/2021.
[89] Ibrahim Ala'A. After Harvey, another mammoth challenge for flooded areas: getting rid of mountains of trash. The Texas Tribune; 2017.
[90] Schwartz John, Blinder Alan. An enormous, urgent task: hauling away Harvey's debris. New York Times; 2017.
[91] Henry Devanandham, Ramirez-Marquez Jose Emmanuel. Generic metrics and quantitative approaches for system resilience as a function of time. Reliab Eng Syst Saf 2012;99:114–22.
[92] NOAA. Major hurricane Harvey - august 25-29, 2017. National Oceanic and Atmospheric Administration, National Weather Service; 2017.
[93] Esmalian Amir, Dong Shangjia, Coleman Natalie, Mostafavi Ali. Determinants of risk disparity due to infrastructure service losses in disasters: a household service gap model. Risk Anal 2019.
[94] Esmalian Amir, Dong Shangjia, Mostafavi Ali. Susceptibility curves for humans: Empirical survival models for determining household-level disturbances from hazards-induced infrastructure service disruptions. Sustainable Cities Soc 2021;66:102694.
[95] Gao Jianxi, Buldyrev Sergey V, Stanley H Eugene, Xu Xiaoming, Havlin Shlomo. Percolation of a general network of networks. Phys Rev E 2013;88(6):062816.
[96] Dong Shangjia, Yu Tianbo, Farahmand Hamed, Mostafavi Ali. Probabilistic modeling of cascading failure risk in interdependent channel and road networks in urban flooding. Sustainable Cities Soc 2020;62:102398.
[97] Tornyeviadzi Hoese Michel, Owusu-Ansah Emmanuel, Mohammed Hadi, Seidu Razak. A systematic framework for dynamic nodal vulnerability assessment of water distribution networks based on multilayer networks. Reliab Eng Syst Saf 2022;219:108217.
[98] Bellè Andrea, Zeng Zhiguo, Duval Carole, Sango Marc, Barros Anne. Modeling and vulnerability analysis of interdependent railway and power networks: Application to british test systems. Reliab Eng Syst Saf 2022;217:108091.